Electroluminescence studies for CYGNO – Directional Dark Matter search with an optical TPC

Cristina M. B. Monteiro

University of Coimbra

F. D. Amaro, E. Baracchini, L. Benussi, S. Bianco, C. Capoccia, M. Caponero, G. Cavoto, A. Cortez, R. J. da Cruz Roque, I. A. Costa, E. Dané, E. Di Marco, G. D'Imperio, G. Dho, F. Di Giambattista, R. R. M. Gregorio, F. Iacoangeli, H. P. Lima Júnior, G. Maccarrone, R. D. P. Mano, M. Marafini, G. Mazzitelli, A. G. Mc Lean, A. Messina, M. L. Migliorini, R. A. Nóbrega, A. Orlandi, I. F. Pains, E. Paoletti, L. Passamonti, F. Petrucci, S. Pelosi, S. Piacentini, D. Piccolo, D. Pierluigi, D. Pinci, A. Prajapati, F. Renga, F. Rosatelli, A. Russo, J. M. F. dos Santos, G. Saviano, A. da Silva Lopes Júnior, N. Spooner, R. Tesauro, S. Tomassini, S. Torelli

CYGNO   INITIUM   1290 UNIVERSIDADE D COIMBRA   LIBPhys-UC

Outline:

- ❑ Electroluminescence : Former studies
- ❑ Detector: Gaseous Counter + GEM + LAAPD
- ❑ Electroluminescence (EL) ➡ scintillation amplification of charge signal

  (Advantages of /requirements for EL)
- ❑ Gas mixtures for CYGNO : CF4, He/CF4, HE/CF4/iso-butane
- ❑ Future work

Electroluminescence : Former studies

Studies of electroluminescence yield (number of photons / primary electron/unit path length)

In different electric field geometries:

- **uniform electric field**: parallel grids;
- **non-uniform electric field:** avalanche-generated EL in very high fields inside the holes of GEM, THGEM, MHSP, MicroMegas;

In pure nobel gases and their mixtures:

- Ar, Xe, Kr, Xe-He, Ne-Xe, Ar-Xe

In mixtures with molecular gases :

- CF4;
- Xe-CF4, Xe-CH4, Xe-CO2, P10

@C.M.B. Monteiro et al., *Secondary scintillation yield in* ***pure xenon***, 2007 JINST 2 P05001

@C.M.B. Monteiro et al., *Secondary scintillation yield in* ***pure argon***, Phys. Lett. B 668 (2008) 167-170

@A.F.M. Fernandes et al. *Low-diffusion* ***Xe-He*** *gas mixtures for rare-event detection: Electroluminescence Yield*, JHEP 04 (2020), 034;

@A. S. Conceição et al., ***GEM*** *scintillation readout with avalanche photodiodes*, 2007 JINST 2 P09010

@C. M. B. Monteiro et al., *Secondary scintillation yield from gaseous* ***micropattern electron multipliers*** *in direct Dark Matter detection*, Phys. Lett. B 677 (2009) 133-138

@C.M.B. Monteiro et al., *Secondary scintillation yield from* ***GEM*** *and* ***THGEM*** *gaseous electron multipliers for direct dark matter search,* Phys. Lett. B 714 (2012) 18-23

@H. N. da Luz et al., ***GEM*** *Operation in High-Pressure* CF_4*: Studies of Charge and Scintillation Properties*, IEEE TNS 56 (2009) 1564 - 1567

@C.A.O. Henriques, et al., *Electroluminescence* ***TPC****s at the thermal diffusion limit*, JHEP 01 (2019) 027. (**xenon** with **CO2**, **CH4** and **CF4**)

@C.A.O. Henriques et al., *Secondary scintillation yield of Xenon with sub-percent levels of* ***CO2 additive*** *for rare event detection,* Phys. Lett. B 773 (2017) 663-671

Detector - 1

- Lab-sized prototype:
- stainless steal chamber,
- indium sealed,
- gas purification / recycling system, with non-evaporable getters, SAES st707, operated at [80,200] ºC, (CF_4 : 150ºC hydrocarbon gases: 80ºC),
- low outgassing materials,
- achieves P ~10^{-6} bar, prior to filling with ultra-pure gases;
- LAAPD (16-mm in diameter) as photosensor for EL readout,

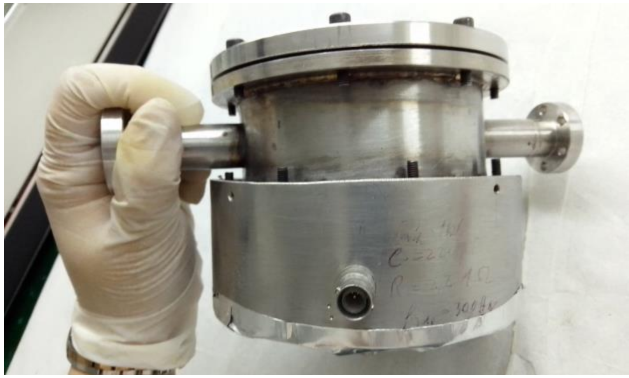

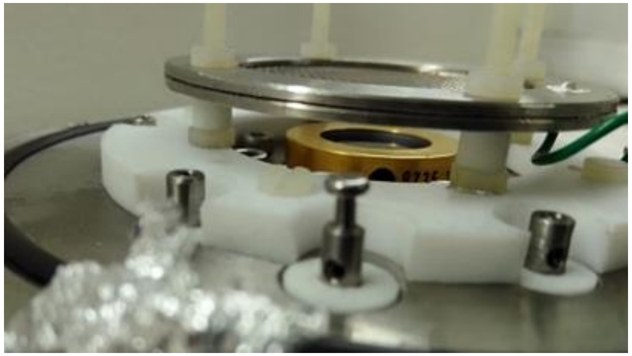

Detector - 2

For these studies the detector has been transformed to flow-mode

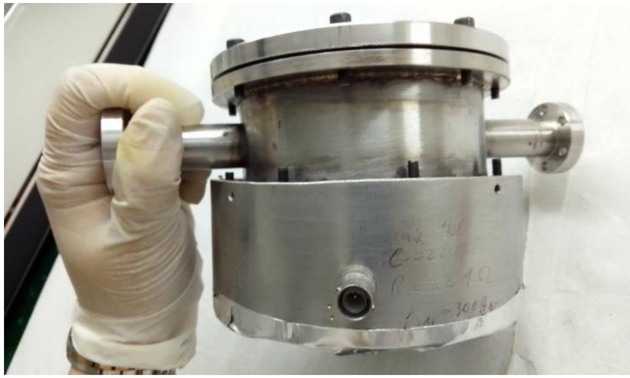

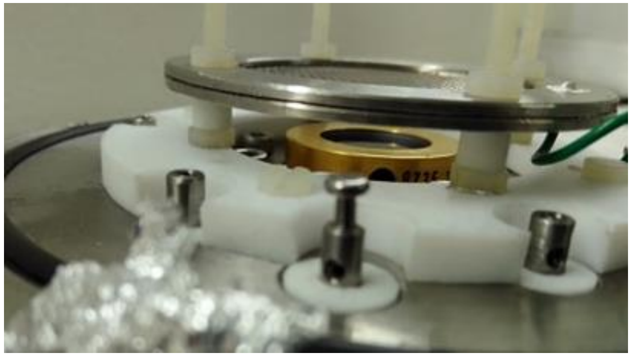

Modified for flow mode:

- Viton seal
- No vacuum before filling
- Getter-purification system removed (flow mode)

Mesh

Mesh made of stainless steel wires (80 micron in diameter) with 900 micron spacing

↓

84% optical transmission.

GEM:

- A standard GEM (50 micron thick, 2.9 x 2.9 cm^2) was used

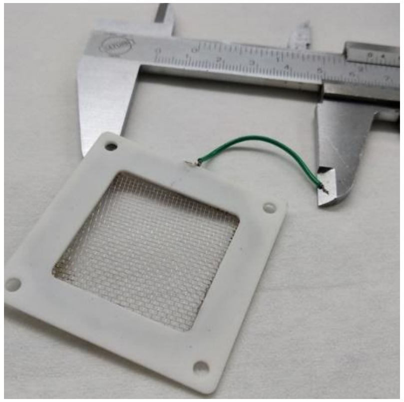

Detector - 3

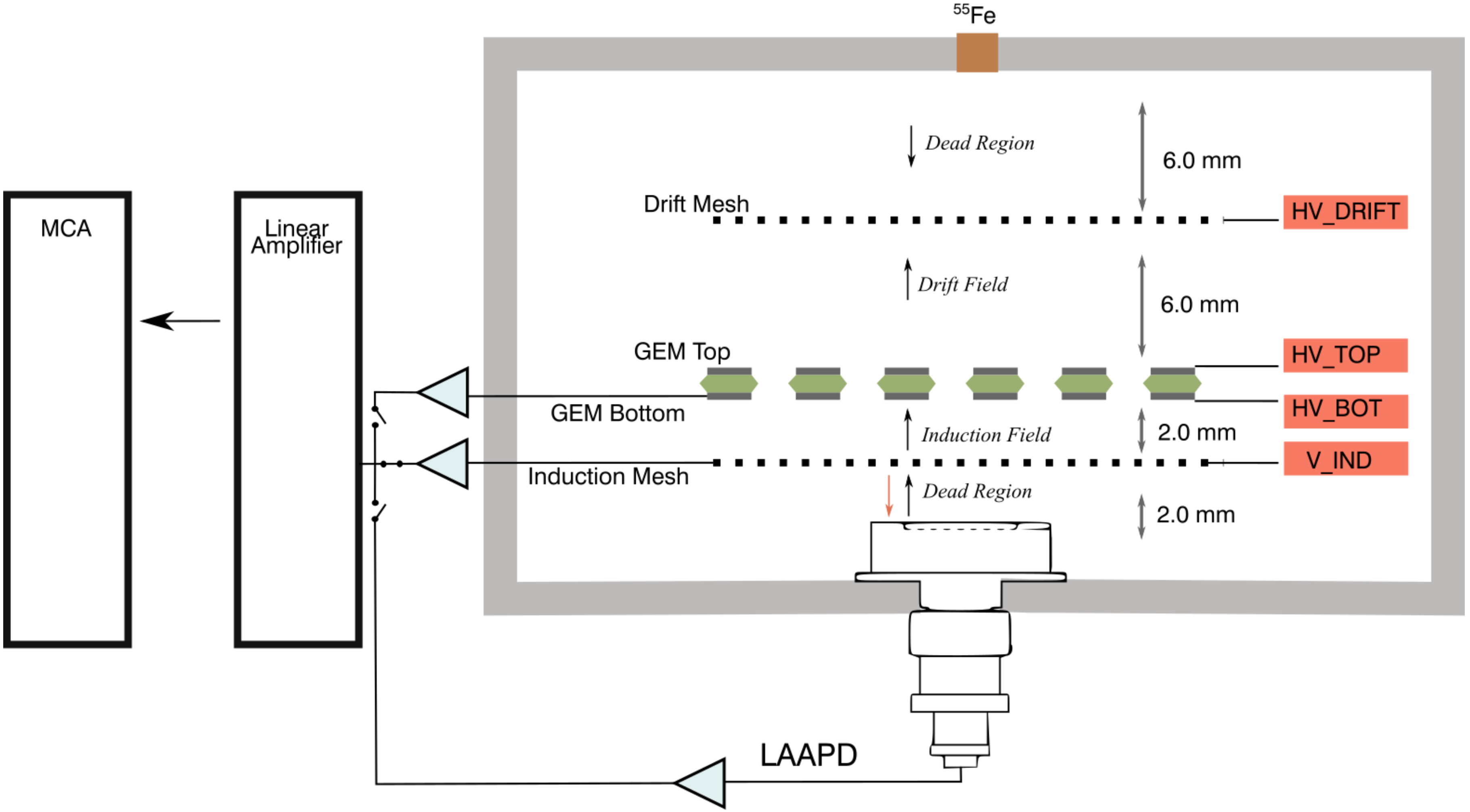

^{55}Fe
Dead Region
6.0 mm
Drift Mesh
HV_DRIFT
MCA
Linear Amplifier
Drift Field
6.0 mm
GEM Top
HV_TOP
GEM Bottom
HV_BOT
Induction Field
2.0 mm
Induction Mesh
V_IND
Dead Region
2.0 mm
LAAPD

LAAPD - 1

- LAAPD from API (Advanced Photonicx Instruments)
- 16-mm diameter active area
- SHV connection.

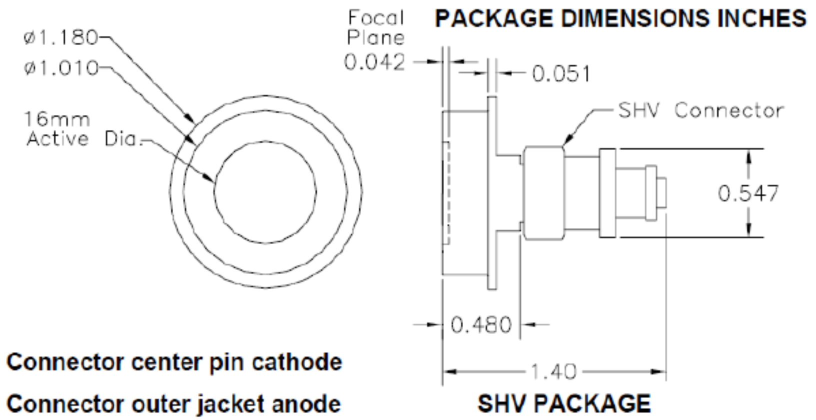

DESCRIPTION

The **SD 630-70-75-500** is a windowless non-cooled large area DUV enhanced silicon avalanche photodiode (APD) with high gain and low noise in a SHV package.

FEATURES

- Low Noise
- High Gain
- High Speed

LAAPD - 2

- LAAPD QE curve : Deep-UV enhanced, but 50-60% in the range [400 - 800] nm
- The LAAPD sensitivity overlaps the one of the ORCA camera (used in CYGNO) in the visible spectrum
- We will use a filter to remove the UV component: an N-BK7 optical window will allow to obtain a similar response as with the ORCA camera.

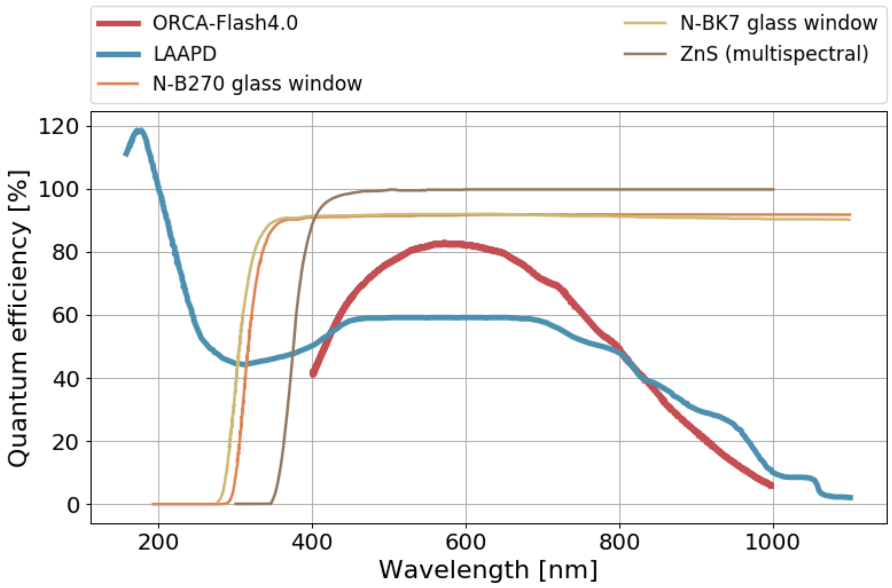

- The optical window is not yet installed in our system
- the results we present cover the spectrum down to the VUV.

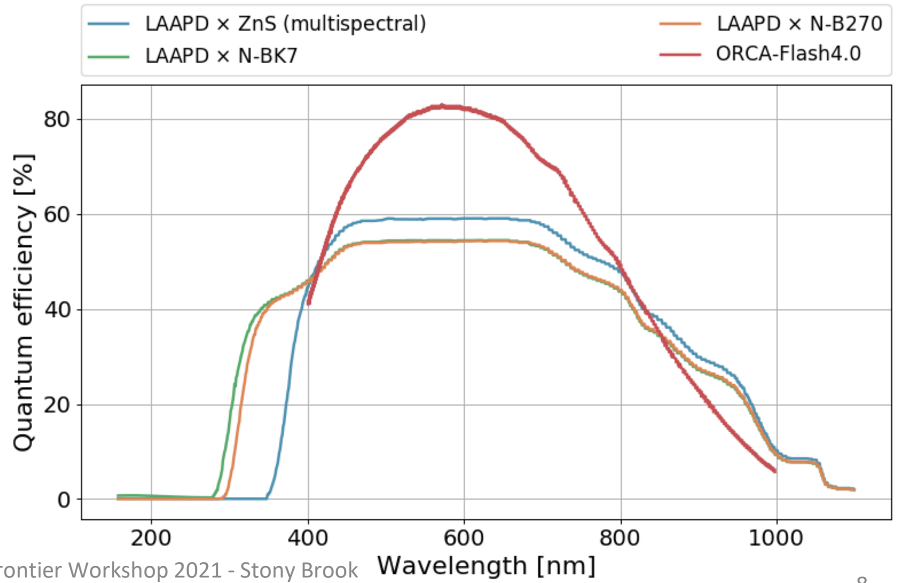

LAAPD - 3

The LAAPD response (orange) comprises two main components:

- x-rays interaction direct in the LAAPD Si-wafer produce a signal, only **dependent on LAAPD biasing** and **independent from the electric field** applied **inside the detector** volume.
  - For a given LAAPD biasing, the position of this peak is constant.
- The Electroluminescence (EL) peak: **depends on the GEM voltage** and **electric fields** in the detector.

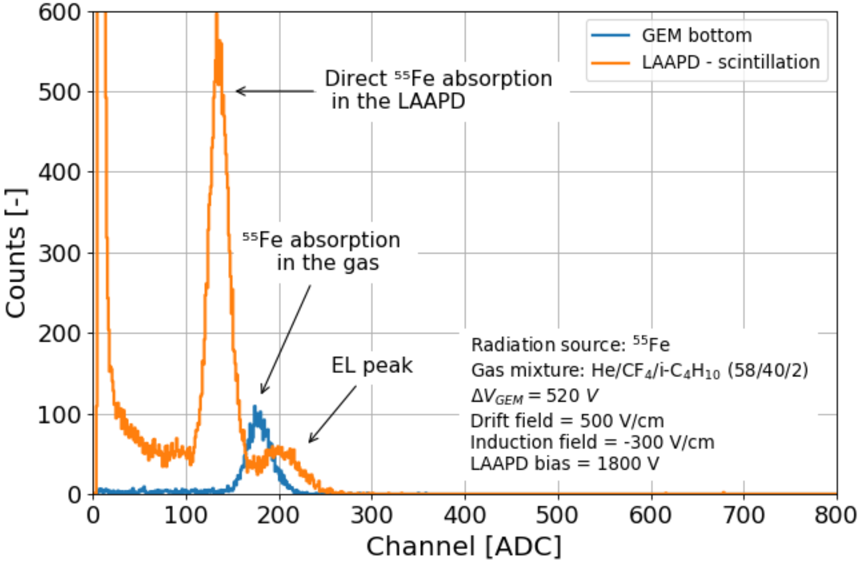

The Absolute Electroluminescence Yield is obtained from these 2 components:

$$Y_{\mathrm{EL}} = \frac{\eta_\gamma}{\eta_{e^-}} = \frac{w(\mathrm{gas})}{w(Si)} \times \frac{A_{EL}}{A_X} \times \frac{1}{QE \times \Omega \times T}$$

[# of photons / primary electron]

A_{EL}, A_X are the centroids of the EL peak and direct x-ray-peak in the LAAPD.
LAAPD-QE used was the value for the plateau at the visible region (0.6)
Ω is the solid angle (0.263) (geometry factor)
T is the mesh transparency (~84%)

CF_4 - Drift Region Optimization

The charge gain measured in the GEM continues to increase with drift field value for longer than anticipated (no plateau).

The El yield (LAAPD) follows the same behavior (due to its dependence on the number of photons produced in the avalanche).

? decrease in e- attachment during drift ?

Signal-to-noise ratio is worse for EL

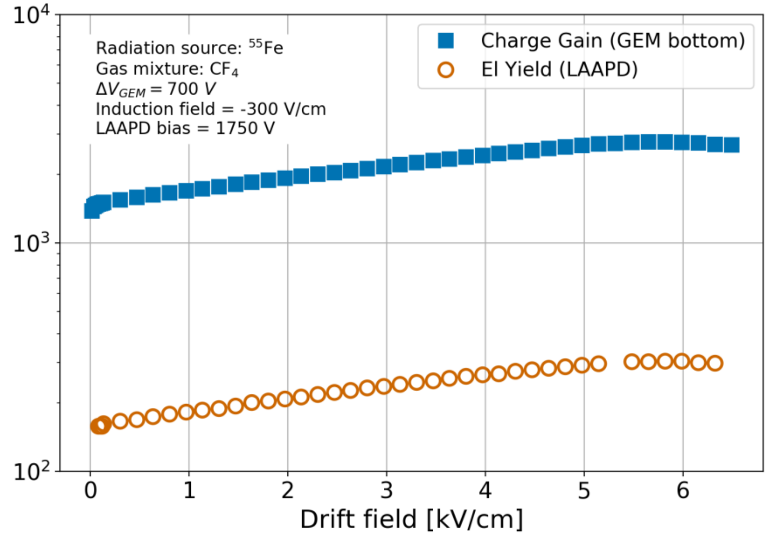

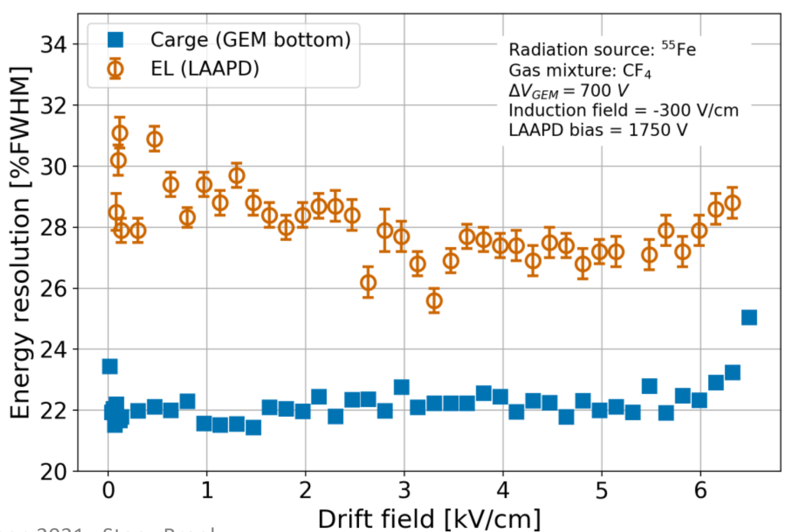

CF_4 vs P10

During the drift region optimization we encountered a unexpected behavior:

Tested with P10: a well-known, "well-behaved" gas

A test with **P10** showed the expected **typical behavior (plateau) – no attachment !**

Preliminary Conclusion: the "odd behavior" is indeed connected to CF_4 electron attachment (and not some issue with the detector).

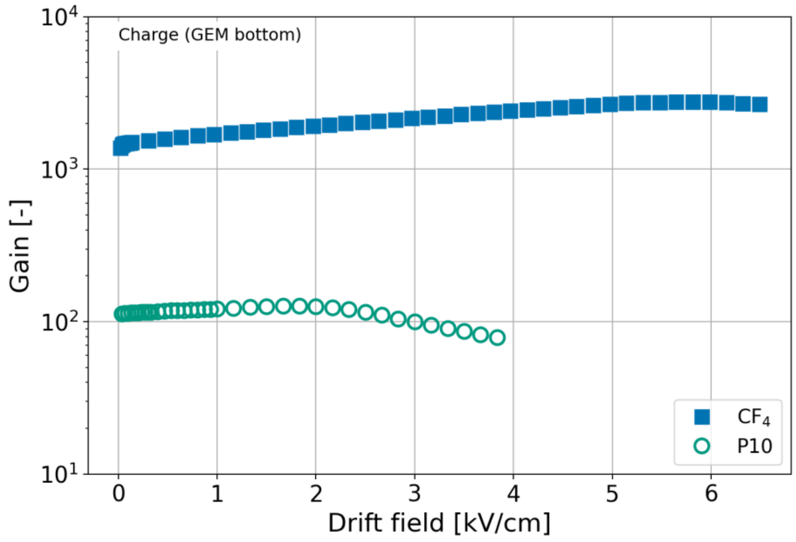

CF_4 – charge gain & EL gain & ER

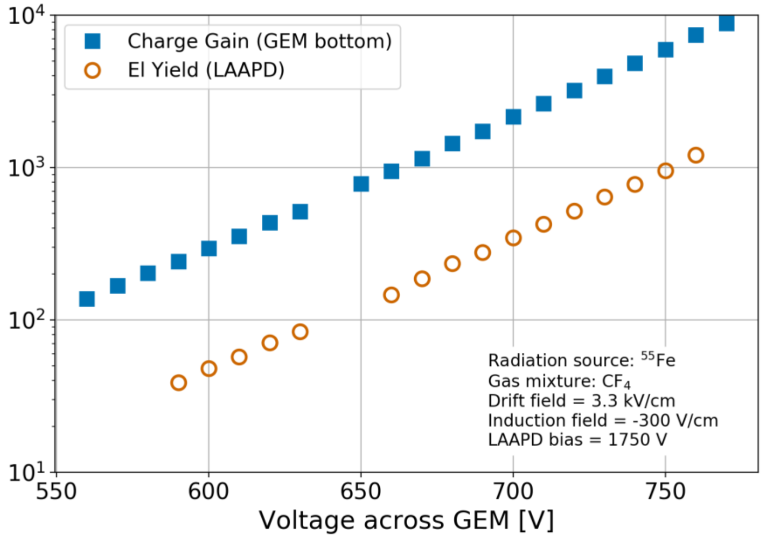

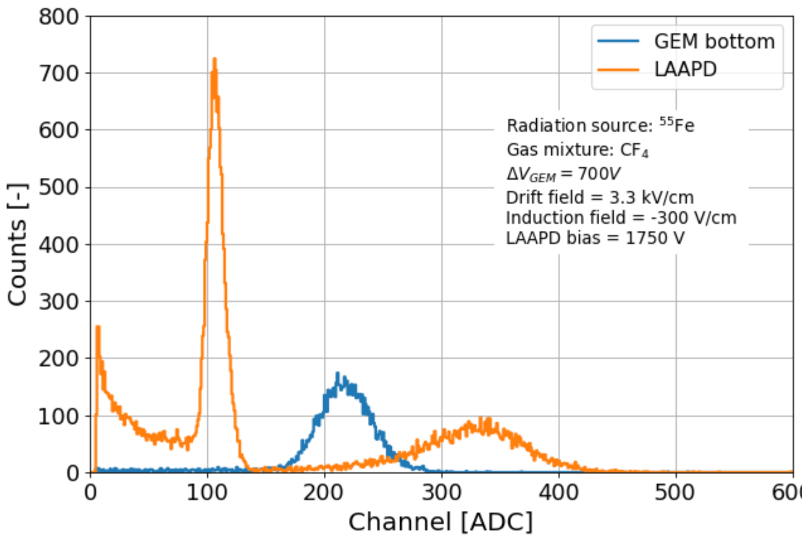

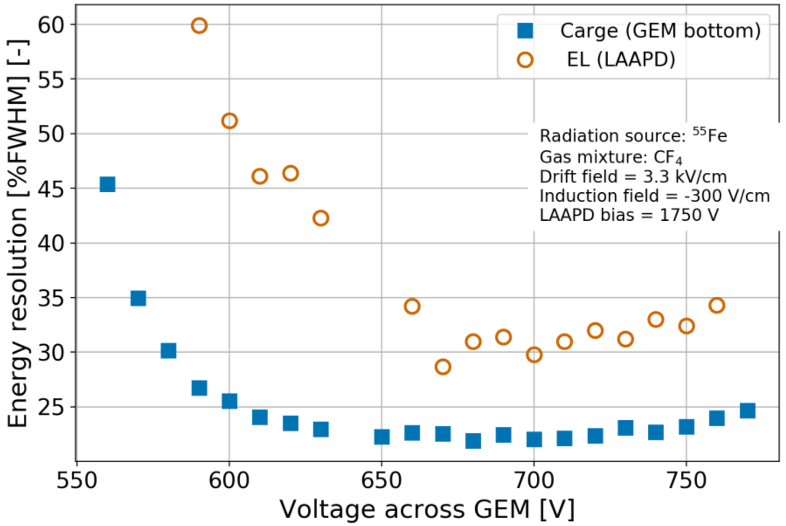

CF_4- Induction field

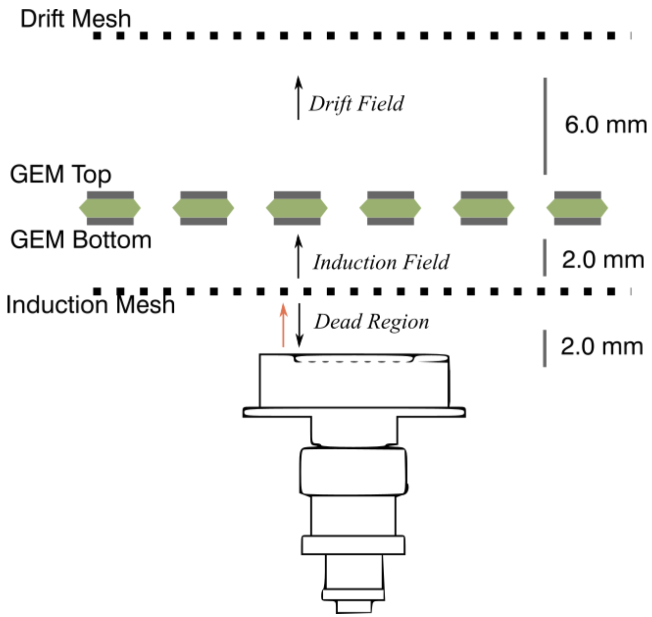

Previous results were taken with a negative (in respect to the fig.) Induction field, to ensure all the charge was collected at the GEM bottom.

We varied the induction field and collected the signals from the GEM bottom and from the Induction Mesh.

The induction field was varied by varying the voltages on the GEM bottom while varying those on the GEM top and Drift Mesh accordingly (to keep those fields constant).

Another surprise was the behavior of the GEM Bottom signal after 7 kV/cm: showing an increase (?)

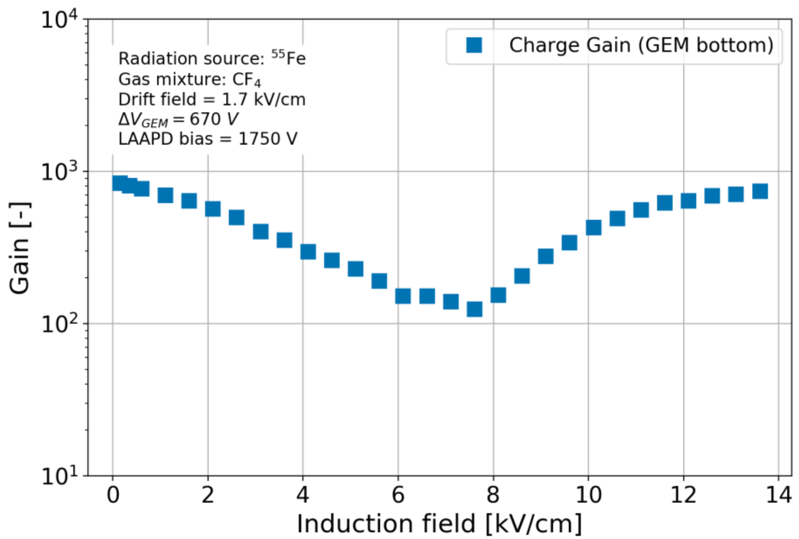

CF_4 - Induction field

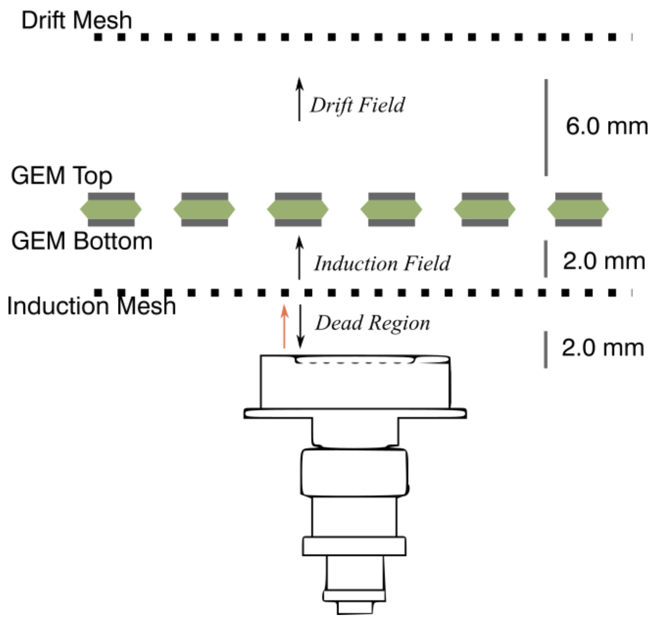

Previous results were taken with a negative (in respect to figure) Induction field, to ensure all the charge was collected at the GEM Bottom.

For this study, we vary the induction field and collect the signals on the GEM Bottom and on the Induction Mesh.

The induction field was changed by changing the voltages on the GEM Bottom while also changing the ones on GEM Top and Drift Mesh (to keep those fields constant).

Another surprise was the behavior of the GEM Bottom signal after 7 kV/cm: showing an increase (?)

For the same region of Induction Field, the signal from the induction mesh, which as expected had been increasing, **started to present a drop**.

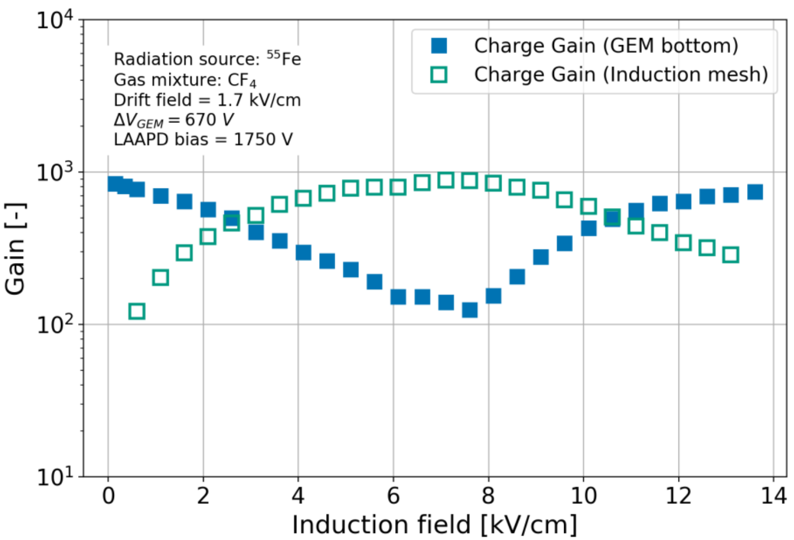

CF_4 - Induction field

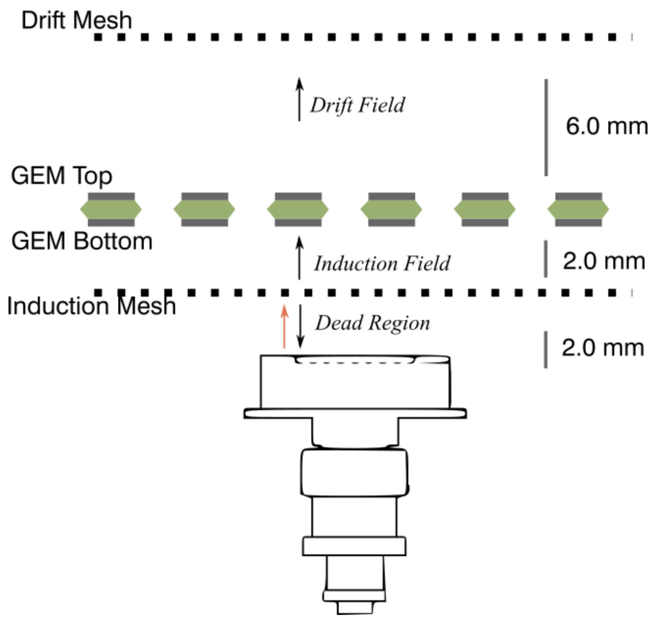

Previous results were taken with a negative (in respect to figure) Induction field, to ensure all the charge was collected at the GEM Bottom.

For this study, we vary the induction field and collect the signals on the GEM Bottom and on the Induction Mesh.

The induction field was changed by changing the voltages on the GEM Bottom while also changing the ones on GEM Top and Drift Mesh (to keep those fields constant).

Another surprise was the behavior of the GEM Bottom signal after 7 kV/cm: showing an increase (?)

For the same region of Induction Field, the signal on the induction mesh, which as expected had been increasing, started to present a drop.

The sum of the 2 components (total charge) increasing slightly (log-scale).

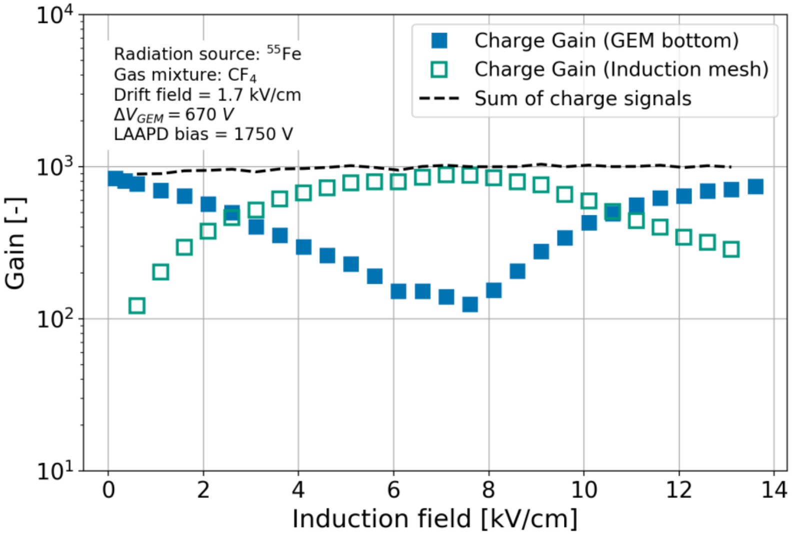

CF_4 - Induction field

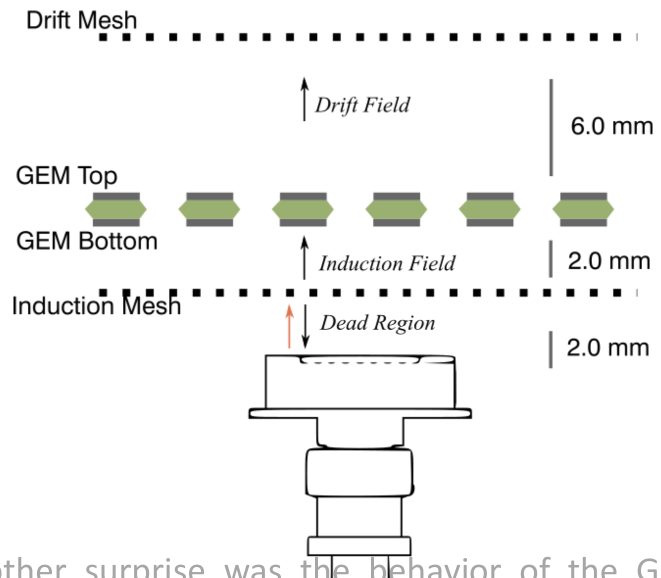

Previous results were taken with a negative (in respect to figure) Induction field, to ensure all the charge was collected at the GEM Bottom.

For this study, we vary the induction field and collect the signals on the GEM Bottom and on the Induction Mesh.

The induction field was changed by changing the voltages on the GEM Bottom while also changing the ones on GEM Top and Drift Mesh (to keep those fields constant).

Another surprise was the behavior of the GEM Bottom signal after 7 kV/cm: showing an increase (?)

For the same region of Induction Field, the signal on the induction mesh, which as expected had been increasing, started to present a drop.

The sum of the 2 components (total charge) increasing slightly (log-scale).

Electroluminescence Yield increases (log-scale) ~50% from 1 kV/cm to ~ 14 kV/cm

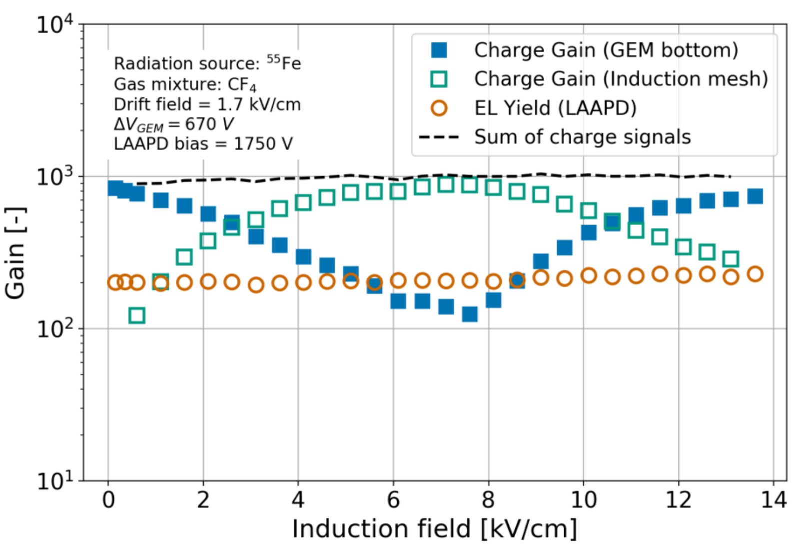

CF_4 vs P10 - Induction field (cross-check)

The behavior in P10 was very different and was as expected:

- The signal on the GEM bottom decreases in amplitude with the increase in the induction field
- The signal on the induction mesh increases steadily.
- **Above 7 kV/cm, we observe some EL with the LAAPD**

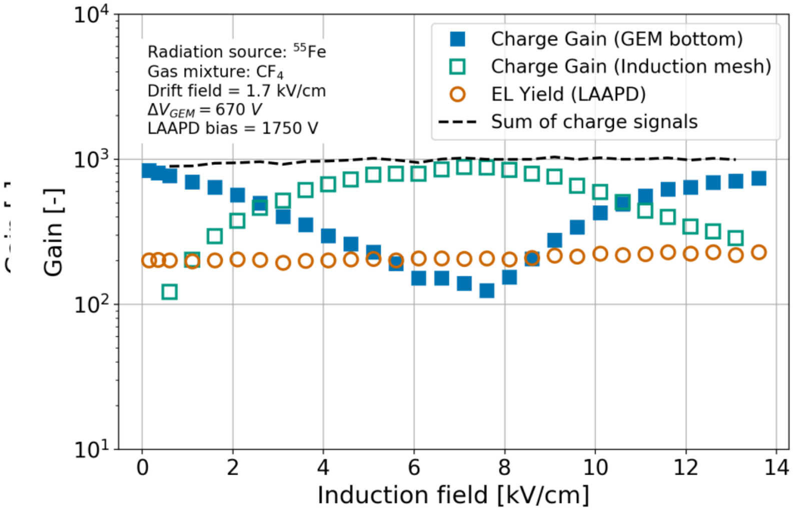

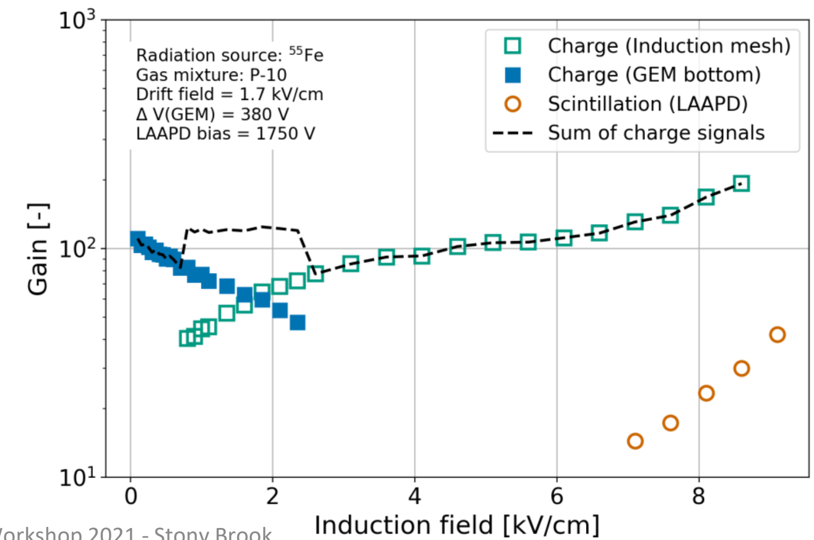

Detector OK!
CF4 behavior odd!
(diffusion and drift velocity variation
+ electron attachment)

He/CF_4 (60/40)- Induction field

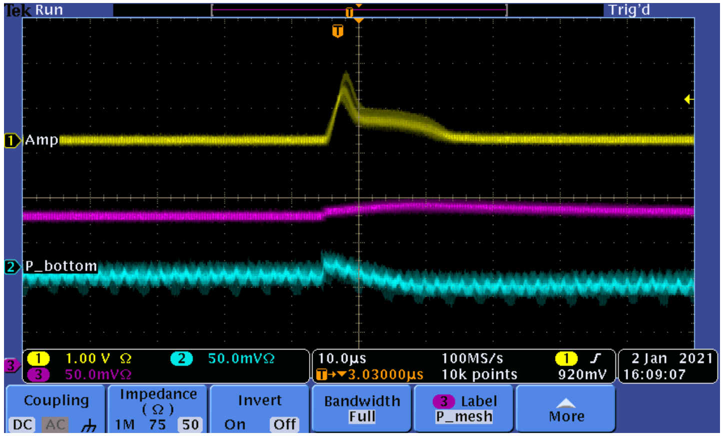

Are ions contributing to signal behavior at higher induction fields?

Gem Bottom = inverse polarity

Mesh = similar polarity

More detailed studies will be done

Integration time: 2 μs

Integration time: 4 μs

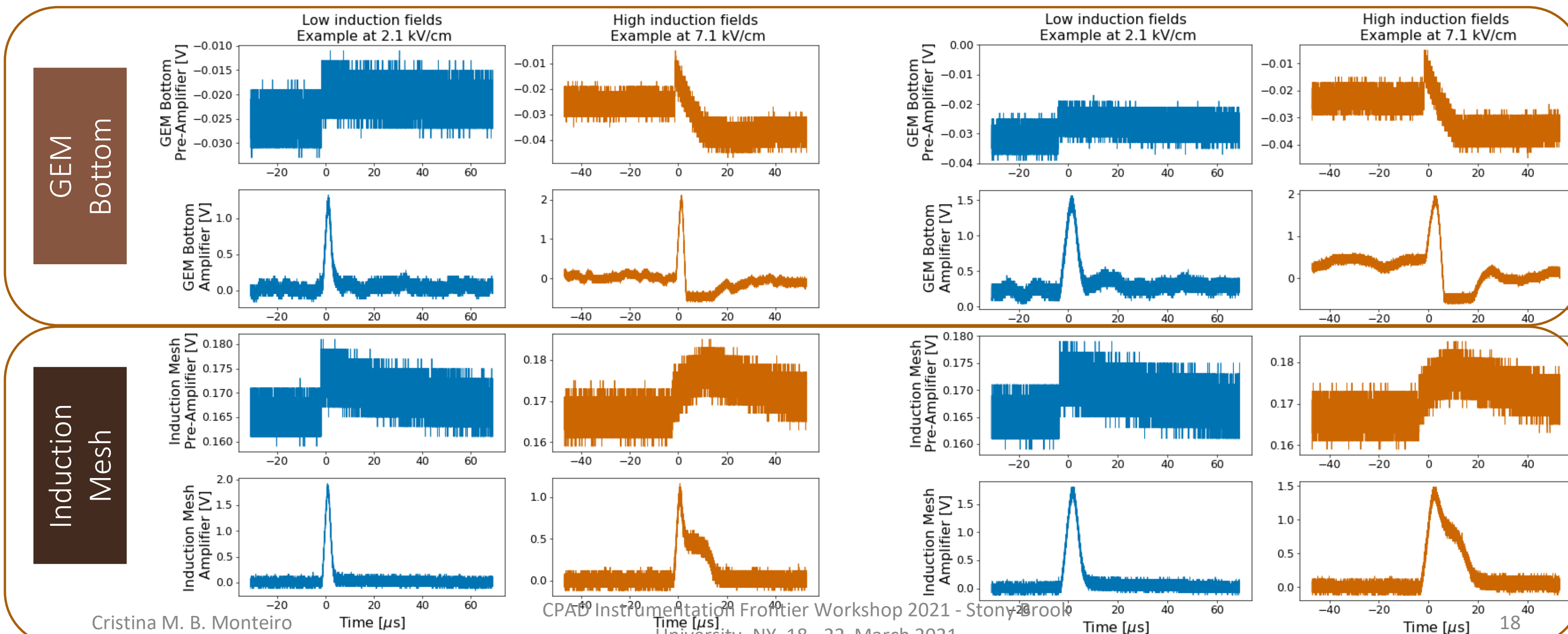

He/CF_4 (60/40) vs CF_4 - Gain & ER

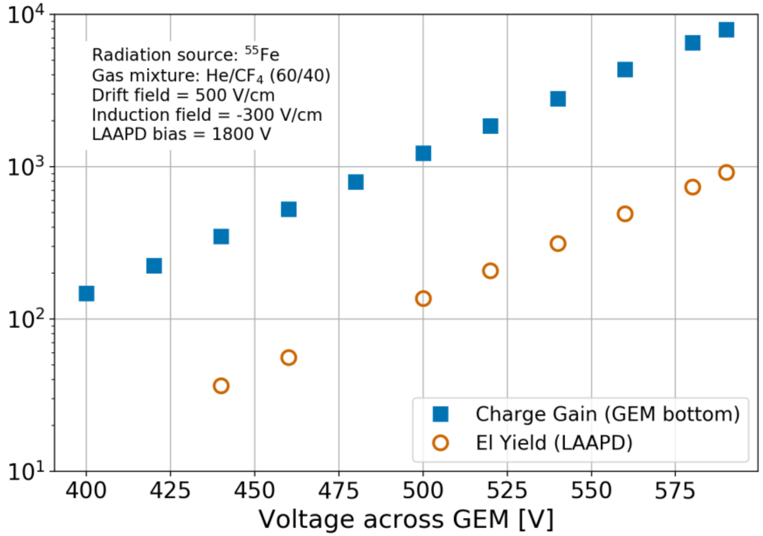

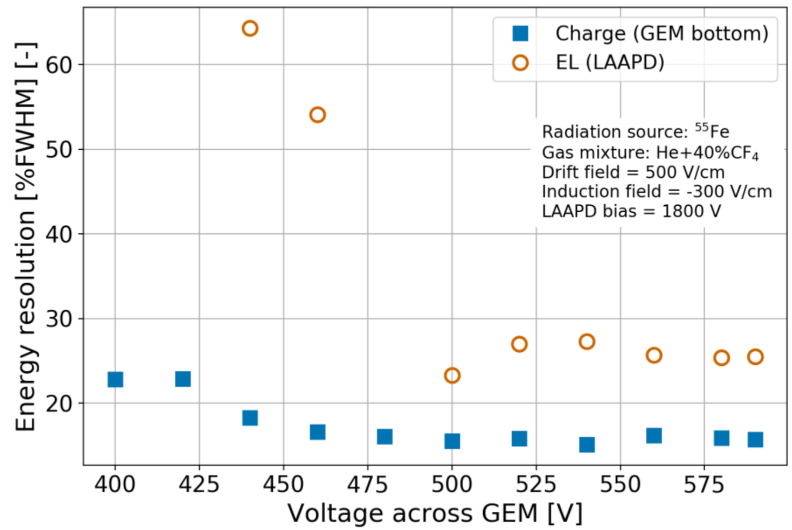

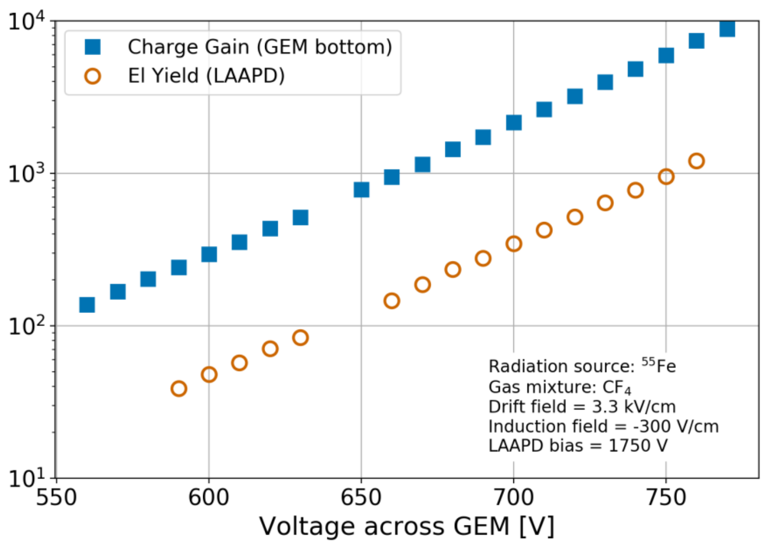

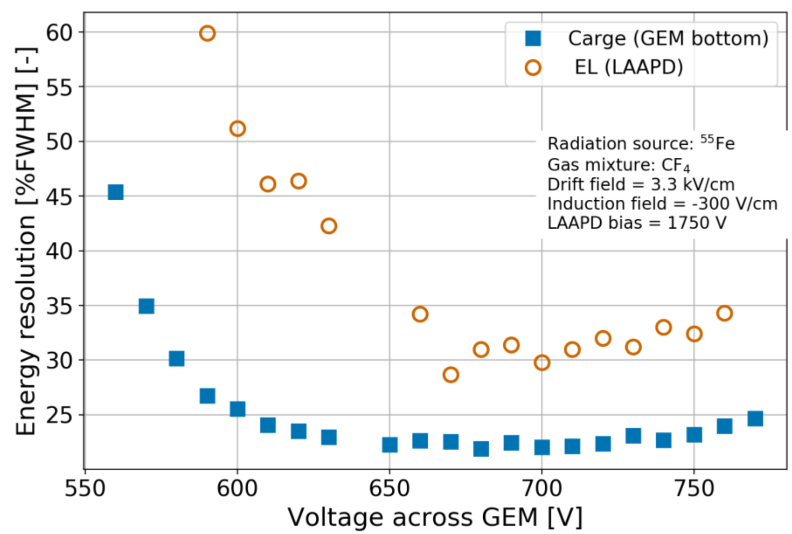

He/CF_4/Iso-Butane (58/40/2)

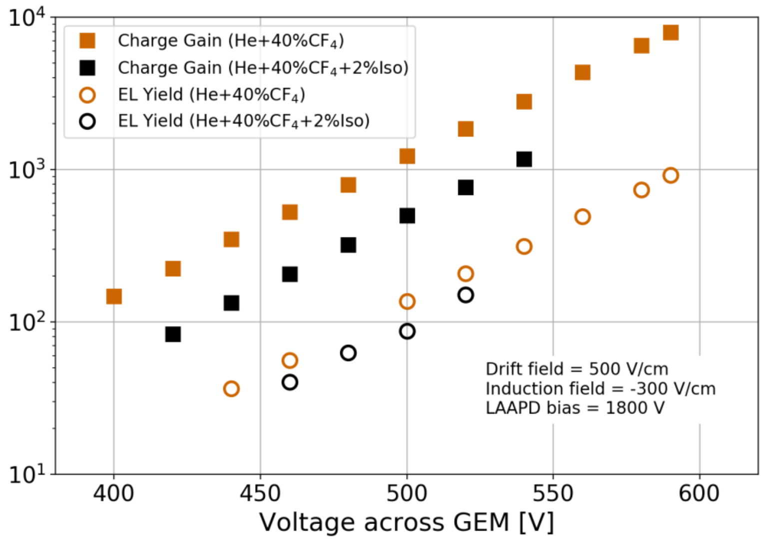

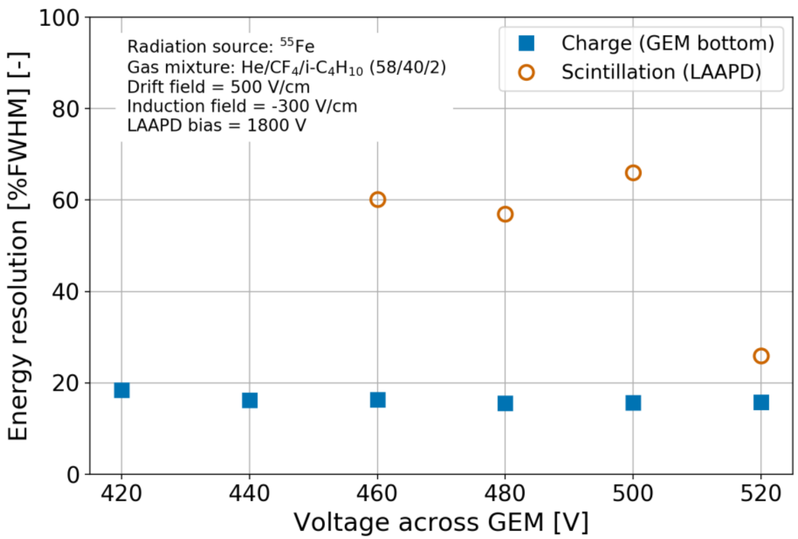

Onset of discharges sooner with the inclusion of Iso-butane

For same charge gain, higher EL yield in He/CF4/Iso (58/40/2)

Future work (already ongoing):

- Increasing **iso-butane %** in the He/CF_4/iso mix
- Investigate **behavior** of the GEM bottom and induction mesh signals **in CF_4 mixtures** with drift and induction fields (ions contributing to signal?)
- Improve **detector insulation** in order to achieve **higher induction fields**
- Include optical glass window for **VUV component removal**
- Return to **operation in sealed mode** (using getters)

This will greatly increase Electroluminescence Yield
And improve Energy Resolution

Acknowledgements

INITIUM Project has received funding from the European Research Council (ERC) under the European Union's Horizon 2020 programme (grant agreement No 818744)

In synergy with

CYGNO Project receives funding from INFN

This work is funded by FEDER, through the Programa Operacional Factores de Competitividade — COMPETE and by National funds through FCT — Fundação para a Ciência e Tecnologia, Portugal, in the frame of project UID/FIS/04559/2020 (LIBPhys).

Thank you for listening !

He/CF_4 (60/40)

E_{IND} = 2.1 kV/cm

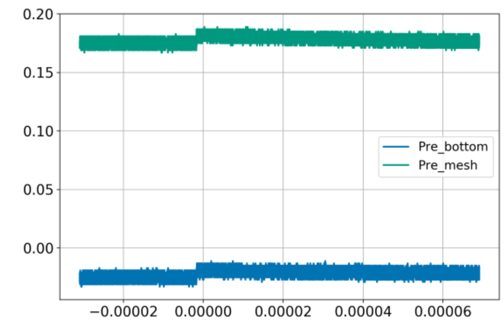

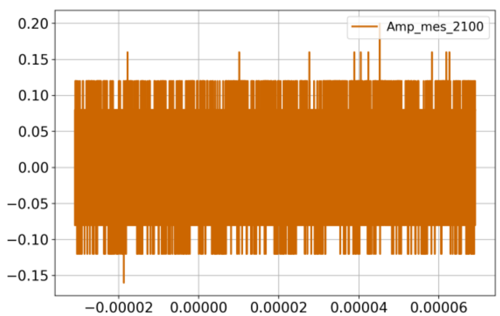

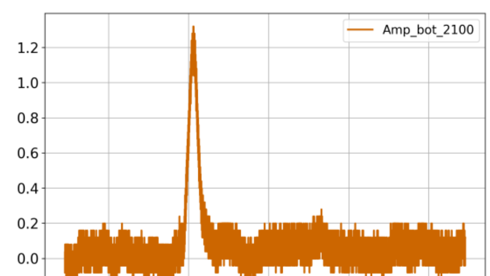

E_{IND} = 5.1 kV/cm

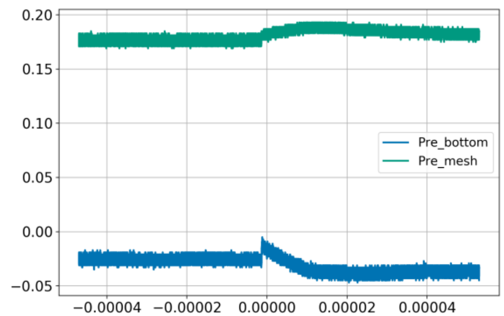

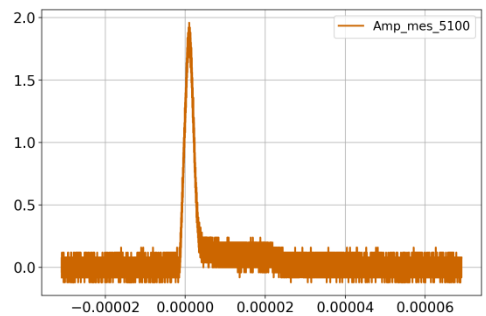

E_{IND} = 7.1 kV/cm